SPECTROPHOTOMETRIC ANALYSIS OF RHEA SURFACE SCATTERING PROPERTIES. M. Ciarniello[1], F. Capaccioni [1], G. Filacchione[1], A. Coradini[2], P. Cerroni[1], F. Tosi[2], K. Stephan[3]. [1]INAF–IASF, via del Fosso del Cavaliere 100, 00133, Rome, Italy, mauro.ciarniello@iasf-roma.inaf.it; [2]INAF–IFSI, via del Fosso del Cavaliere 100, 00133, Rome, Italy; [3] Institute of Planetary Research, DLR - German Aerospace Center, Rutherfordstrasse 2, D-12489, Berlin, Germany.

Introduction: The large amount of data from VIMS (Visual Infrared Mapping Spectrometer) onboard Cassini spacecraft allows to study the surface properties of the icy bodies of the Saturnian system under various geometry configurations and in a spectral range extending from 0.35 μm to 5.1 μm. In particular, we have collected 2500 disk integrated observations of the satellites, which represent a statistically significant dataset [1,2].

The variability of the spectra has been empirically analysed in [1,2] using various "spectral indicators" (such as spectral slopes, band depth, continuum level, etc.) and their relationships. The goal of this work is to provide a quantitative evaluation of the parameters that contributes to the spectrophotometric properties of the surface materials. A powerful mean to infer information on the composition and on the surface properties of the satellites is the modeling of the spectra and of the phase functions by means of radiative transfer equations, as for instance given in [3].

Object of this study is Rhea, the second largest satellite of the system; among the available disk integrated observations we have selected a dataset composed of 112 hyperspectral full-disk spectra of the moon leading side, acquired in a range of phase angles extending from 0° up to 110°.

Applying the Hapke model [3] we fitted both spectra and phase functions, constraining the amount of organic contaminants in the water ice covering the surface, the particle size, the surface roughness and the opposition effect surge. From the spectral fits we obtained a typical grain size of 40 μm with a small percentage of tholin (less than 1%) embedded in the ice particles. The study of phase function shows that both Shadow Hiding and Coherent Backscattering contribute to the opposition effect.

Shape of the spectrum and phase angle: The spectra of Rhea exhibit typical features of water ice, with strong absorption bands at 1.5 μm, 2.0 μm and 3.0 μm. The shape of the spectra depends on the geometry of the observation, in figure 1 is shown a collection of spectra taken at increasing phase angles and normalized at 1.8 μm. The spectra show a progressive reddening with increasing phase angle as well as an enhancement of the water ice absorption band depths (Fig. 1). It is interesting to note that above 3 μm the trend is reversed showing a decrease of the reflectance with phase.

Phase reddening is common for non icy body, such as Mercury and the Moon [4], but has not a clear explanation. On the other side band depth enhancement with phase angle can be interpreted as an increasing contribution of multiple scattering that dominates on the wings of the band respect to the single scattering which is predominant in the center of the band.

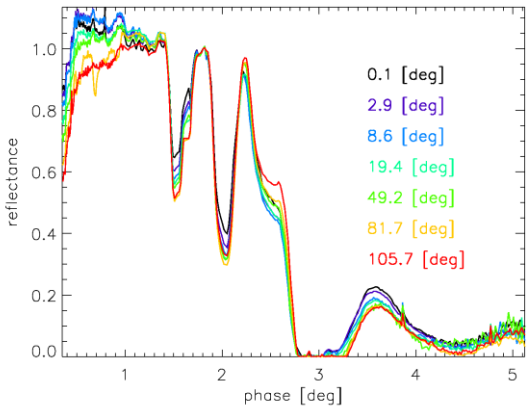

Figure.1: Full-disk spectra of Rhea normalized at 1.8 μm for various phase angles (indicated in the plot).

Spectral fit: Using the Hapke's spectral model we fitted Rhea's spectra at different phase angles in order to estimate the particle size of the water ice grains covering the surface, the amount of crystalline and amorphous phase and the percentage of organic contaminants. In our modelization we used water ice particles characterized by a monodisperse grain size distribution with intramolecular inclusions of organic compounds (tholin), following the approach given in [5,6]. Optical constants for water ice measured at a range of temperature of interest for the Saturn satellites are from [7,8,9] while for tholin from [10]. Intramolecular mixing (instead of areal mixing or intimate mixing) is the only one able to reproduce the strong reddening of the spectrum towards 350 nm. A typical fit is presented in Fig. 2. In this case we show an intramolecular mixture of water ice with 0.8% tholins and grains diameter of 42 μm.

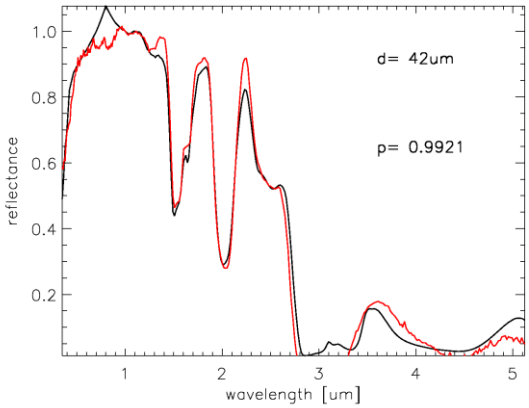

Figure 2: Observed (red) and fitted (black) spectra of Rhea, normalized at 1.00 µm (phase angle = 90°).

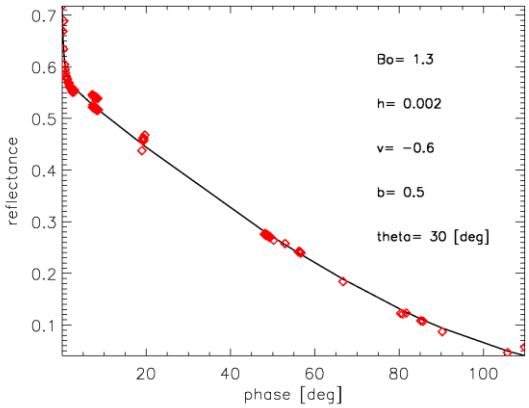

Figure 3: Observed (diamonds) and fitted (black) phase function at 1.8 µm. B_0 and h are respectively the amplitude and width of opposition effect, v and b are the parameters of single particle phase function and *theta* describes large scale surface roughness.

Phase function fit: We fitted the phase function of Rhea at different wavelengths, and we retrieved the bidirectional reflectance parameters applying the Hapke model. As an example the phase curve obtained at the wavelength of 1.8 µm is shown in Fig.3.

The broad phase angle coverage allows to study the opposition effect surge (Shadow Hiding -SH- or Coherent Backscatter -CB- opposition effect) as well as the multiple scattering tail of the phase function, retrieving information about the particles agglomeration and the large scale surface roughness of the satellite. To model the opposition effect surge we used the analytical expression for Shadow Hiding with the possibility for the parameter B_0 that describes the effect amplitude to be greater than 1 in order to take into account for additional coherent backscattering [4].

Figure 3 reports the values of the parameters fit; the B_0 value is indicative of the shared contribution of SH and CB to the opposition effect. Additionally, the very small value for the opposition effect width (h) is consistent with the very narrow peak observed at this wavelength.

Acknowledgments: This work is supported by an Italian Space Agency (ASI) grant.

References: [1] Filacchione, G. et al, (2007) *Icarus*, 186, 259-290. [2] Filacchione G. et al. (2010) *Icarus*, in press. [3] Hapke B. (1993) *Theory of reflectance and emittance spectroscopy*, Cambridge Univ. Press, New York. [4] Warrell J. and Bergfors (2008) *Planetary and Space Science*, *56*, 1939-1948. [5] Wilson, P.D. et al, (1994) *Icarus*, 107, 288-303. [6] Cruikshank, D.P. et al. (2005) *Icarus*, 175, 268-283. [7] Mastrapa R. M. et al. (2009) *The Astrophysical Journal*, *701*, 1347–1356. [8] Warren S. G. (1984) *Applied Optics, 23 (n.8)*, 1206-1225. [9] Grundy W. M. and Schmitt B. (1998) *J. Geophys. Res., 103(E11)*, 25.809–25.822. [10] Khare B. N. et al (1993) *Icarus*, *103*, 290-300.